Scientific Research Publishing

Open Journal of Radiology, 2025, 15(1), 1-12
https://www.scirp.org/journal/ojrad
ISSN Online: 2164-3032
ISSN Print: 2164-3024

Retrospective Study of Bone Mineral Density through Phantom-Less Quantitative CT

Hongmin Xu, Alexander Kui, Alice Barrington, Emad Allam, Jian-Feng Chen*

Department of Radiology and Medical Imaging, Stritch School of Medicine, Loyola University Medical Center, Chicago, IL, USA
Email: *jfchen@live.com

How to cite this paper: Xu, H.M., Kui, A., Barrington, A., Allam, E. and Chen, J.-F. (2025) Retrospective Study of Bone Mineral Density through Phantom-Less Quantitative CT. *Open Journal of Radiology*, **15**, 1-12.
https://doi.org/10.4236/ojrad.2025.151001

Received: December 6, 2024
Accepted: February 7, 2025
Published: February 10, 2025

Abstract

Background: Quantifying bone mineral density (BMD) is important to monitor and evaluate bone health status. When applied to chest and abdomen CT images, the BMD values of thoracic and lumbar spines can be determined. **Objective:** This study aims to analyze the distribution of lumbar BMD across different age groups and races, investigate the correlation between lumbar BMD and thoracic BMD, evaluate the feasibility of using chest CT scans for BMD assessment, and analyze numerical data to establish CT-based thresholds for diagnosing osteopenia and osteoporosis. **Methodology:** CT imaging data from 400 female subjects aged 20 - 80 years, acquired from 2010 to 2022, was studied retrospectively. We examined variations in lumbar BMD among females across different ages and races. The thoracic BMD values were measured relative to aortic blood and subcutaneous adipose tissue on chest CT images, while the lumbar BMD values were measured relative to psoas muscle and subcutaneous adipose tissue on abdominal CT images. Then, the correlation coefficient of BMD values between thoracic and lumbar was calculated. The receiver operating characteristic (ROC) of thoracic spine BMD values was studied with the lumbar spine BMD values considered the gold standard for osteoporosis diagnosis. **Results:** Thoracic BMD ranged from 60 - 350 mg/cm^3, while lumbar BMD ranged from 60 - 350 mg/cm^3 in most subjects. Between thoracic and lumbar BMD, a strong positive correlation (r = 0.95) was determined and the area under the ROC curve was 0.969. Lumbar BMD demonstrates age-related decline and has a strong positive correlation with thoracic BMD. Among the four major racial groups—White, Black, Hispanic, and Asian—Hispanics exhibited the highest lumbar BMD, while Whites showed the lowest. **Conclusions:** Lumbar BMD demonstrates age-related decline and strongly correlates with thoracic BMD. These findings support the use of CT as a valuable tool in screening for osteoporosis.

Keywords

Quantitative CT (QCT), Bone Mineral Density (BMD), Thoracic BMD, Lumbar BMD, Phantom-Less

1. Introduction

Osteoporosis is a bone disease characterized by low bone mineral density (BMD) and micro-architectural deterioration of bone tissue [1]. BMD measurement by using dual-energy X-ray absorptiometry (DXA) is defined by the World Health Organization (WHO) Working Group as the gold standard and is clinically used to diagnose osteoporosis [2]. BMD is clearly one of the major determinants of bone strength and fracture risk [3]-[5]. Quantitative computed tomography (QCT) has been shown to provide a similar accurate fracture prediction. In QCT, there are two methods to measure the BMD using calibration phantoms. One is called the simultaneous calibration method, in which the subject is scanned on top of a calibration phantom, which contains several inserts of known values of hydroxyapatite (HA) or similar substances characteristic of bone material. Based on the CT values measured in these inserts, CT values measured in the bone can be converted to BMD. This method has the advantage of minimizing the difference in X-ray beam properties between the bone of interest and the inserts of the calibration phantom. Another is called the asynchronous calibration method, where a calibration phantom is measured separately from the subject. This method is suitable for current modern CTs, which have stable performance. This technique requires additional phantom imaging and therefore limits its clinical applicability. All of these phantom-based calibration methods are rarely used in a clinical setting, since they require additional time and clinical resources and produce image artifacts. Instead of using these calibration phantoms, certain tissues called internal calibration materials within the body, such as muscle, blood, and subcutaneous adipose tissue, can be used. It is assumed that the composition of these internal calibration materials does not vary among subjects. The development and validation of internal calibration techniques were defined as a priority by the International Society of Clinical Densitometry [6] to move the field towards clinically implemented skeletal health assessment. Internal density calibration techniques have been in development for several years. However, these techniques, either commercially available or custom-made, rely on the basic assumptions of ground truth values for each calibration tissue. Weaver *et al.* determined the ground truth reference values of −69 mg/cc for fat and 77 mg/cc for muscle and then used these reference values for the internal density calibrations [7]. Similarly, using clinically available CT scanners, the regions of interest (ROI) of subcutaneous fat and paraspinal muscle are selected and used to measure BMD [8] [9]. Furthermore, ROIs of air and blood or fat have also been paired with developed reference values of equivalent BMD to measure bone's BMD [10]. These phantom-less methods have been applied to

abdominal CT images to determine the BMD of lumbar spines [7] [11]. In our study, we applied the phantom-less method to clinical chest and abdominal CT images to determine the BMD of thoracic and lumbar spines. The first step of this study was to determine the reference values of aortic blood in the chest based on a linear model, which can be used to determine BMD values of the thoracic spine. The second step was to determine the thoracic BMD values based on the internal reference tissues of aortic blood and anterior subcutaneous fat located in the chest and determine the lumbar BMD values based on the internal reference tissues of psoas muscle and anterior subcutaneous fat located in the abdomen. The third step was to analyze the correlation between these thoracic and lumbar BMD values.

2. Materials and Methods

2.1. Study Subjects

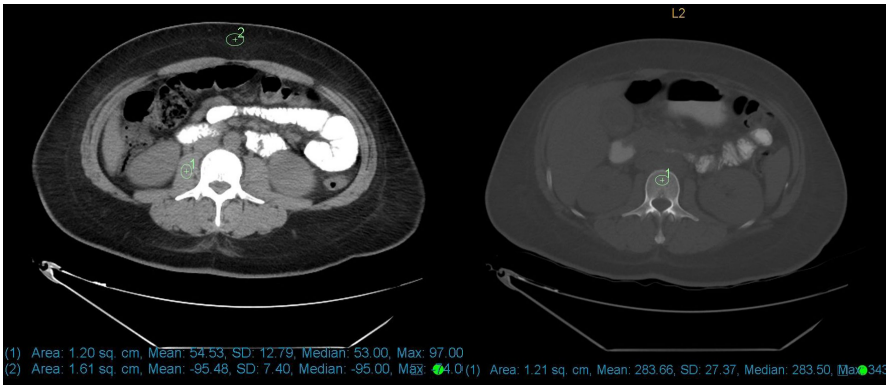

(a) (b)

Figure 1. The mean HU values in three regions of interest (ROI) were measured including right psoas muscle and anterior subcutaneous fat in a soft tissue window for internal calibration, and lumbar vertebrae in the bone window.

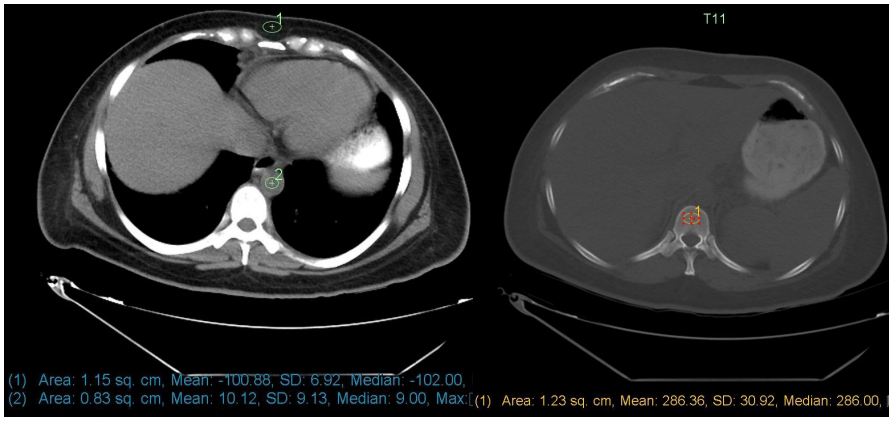

(a) (b)

Figure 2. The mean CT values in three regions of interest (ROI) were measured including aortic blood and anterior subcutaneous fat in a soft tissue window for internal calibration, and thoracic vertebrae in the bone window.

CT images of the chest and abdomen without contrast of 400 females were studied retrospectively. Their ages ranged from 20 to 80 years old with a median age of 59 years old. Exclusions were made for conditions affecting BMD, such as chronic kidney disease, vitamin D deficiency, long-term steroid use, hyperparathyroidism and hyperthyroidism, cirrhosis, acute leukemia, and diffuse spinal metastases. These clinical images were acquired by GE scanners (Revolution, GE Healthcare, Waukesha, WI, USA). The chest and abdomen were scanned using a standard helical imaging protocol (120 kVp, 5.0 mm slice thickness, and standard reconstruction kernel) with exposure set by automatic exposure control. Both thoracic and lumbar vertebral Hounsfield unit (HU) values were measured in the mid-vertebral trabecular region from the T11-L4 vertebrae. The average HU value of the thoracic spine and the average HU value of the lumbar spine were then calculated. Additional measurements were made including the HU values of the anterior subcutaneous fat of the chest and abdomen, right psoas muscle, and aortic blood in the chest (**Figure 1** and **Figure 2**). To enable phantom-less calibration for QCT, aortic blood and psoas muscle were selected as internal calibration references. These tissues were chosen based on their anatomical proximity to the spine [8] [10], consistent composition [6] [8], and stable attenuation properties in CT imaging, as supported by previous studies [6] [9] [10] [12].

2.2. Determination of the Reference Value for Aortic Blood

In this study, the relationship between BMD of soft tissues, such as subcutaneous fat, psoas muscle and aortic blood, and their measured CT HU values are assumed as a linear relationship:

$$BMD = a \times CT + b \tag{1}$$

where the constants a and b are obtained by phantom-less calibration with the ground truth reference values of $BMD_{fat} = -69$ mg/cm^3 for subcutaneous fat and $BMD_{muscle} = 77$ mg/cm^3 for paraspinal muscle:

$$a = \frac{BMD_{muscle} - BMD_{fat}}{\langle CT_{muscle} \rangle - \langle CT_{fat} \rangle} \tag{2}$$

and

$$\begin{aligned} b &= BMD_{muscle} - a\langle CT_{muscle} \rangle \\ &= \frac{BMD_{fat} \times \langle CT_{muscle} \rangle - BMD_{muscle} \times \langle CT_{fat} \rangle}{\langle CT_{muscle} \rangle - \langle CT_{fat} \rangle} \end{aligned} \tag{3}$$

where <…> stands for an ensemble average over N subjects. After determining the constants a and b, the mean BMD value of aortic blood can be calculated by using the HU values of aortic blood, which is $BMD_{aortic\ blood} = 25$ mg/cm^3.

2.3. Calculation of the BMD Values of Thoracic Spines

Then, the values of thoracic BMD can be determined by the HU values of the

thoracic spine vertebrae, aortic blood and anterior subcutaneous fat on chest CT images:

$$BMD_{thoracic\ spine} = \frac{BMD_{aortic\ blood} - BMD_{fat}}{\langle CT_{aortic\ blood}\rangle - \langle CT_{fat}\rangle} \times CT_{thoracic\ spine} + \frac{BMD_{fat} \times \langle CT_{aortic\ blood}\rangle - BMD_{aortic\ blood} \times \langle CT_{fat}\rangle}{\langle CT_{aortic\ blood}\rangle - \langle CT_{fat}\rangle}$$

Similarly, the values of lumbar BMD can be determined by the HU values of the lumbar spine vertebrae, psoas muscle and anterior subcutaneous fat on abdominal CT images:

$$BMD_{lumbar\ spine} = \frac{BMD_{muscle} - BMD_{fat}}{\langle CT_{muscle}\rangle - \langle CT_{fat}\rangle} \times CT_{lumbar\ spine} + \frac{BMD_{fat} \times \langle CT_{muscle}\rangle - BMD_{muscle} \times \langle CT_{fat}\rangle}{\langle CT_{muscle}\rangle - \langle CT_{fat}\rangle}$$

2.4. Statistical Analysis

The Pearson correlation coefficient for the BMD values between thoracic and lumbar spines was calculated. The Pearson correlation coefficient is given by:

$$r = \frac{\sum_{i=1}^{N}\left(X_i - \bar{X}\right)\left(Y_i - \bar{Y}\right)}{\sqrt{\sum_{i=1}^{N}\left(X_i - \bar{X}\right)^2 \sum_{i=1}^{N}\left(Y_i - \bar{Y}\right)^2}} \tag{4}$$

where X_i is the $BMD_{thoracic\ spine}$, Y_i is the $BMD_{lumbar\ spine}$ of the subject *I*, $\bar{X}$ is the mean of $BMD_{thoracic\ spine}$, $\bar{Y}$ is the mean of $BMD_{lumbar\ spine}$, and N is the total number of subjects. Then, linear regression models and their *R*-squared value were also calculated. The *R*-squared value shows how well the data fits the regression model.

The receiver operating characteristic (ROC) of thoracic BMD values was studied with lumbar BMD values considered the gold standard for osteoporosis diagnosis. The area under the ROC curve was used to evaluate the suitability of thoracic BMD values for osteoporosis diagnosis.

3. Results

For the 400 female subjects examined, their ages ranged from 20 to 80 years old. Both thoracic and lumbar vertebral CT HU values were measured in the mid-vertebral trabecular region. Thoracic BMD values ranged from 60 - 350 mg/cm^3, while lumbar BMD values ranged from 60 - 350 mg/cm^3 in most subjects. **Figure 3** and **Figure 4** show the changes in BMD values of the thoracic and lumbar spine with age. These results indicate that spinal BMD gradually decreases with increasing age. The Pearson correlation coefficient between thoracic and lumbar BMD is 0.953 ($p < 0.0001$), and linear regression line with zero intercept shows *R*-squared

value = 0.9893, as shown in Figure 5. These results show that there is a very high correlation between thoracic and lumbar BMD.

For subjects aged 20 - 40, lumbar BMD exhibited a mean of 233 mg/cm^3 and standard deviation of 55 mg/cm^3. A threshold lumbar BMD value of 123 mg/cm^3 corresponded to a T-score of −2 and was closely aligned with ACR guidelines (BMD > 120 mg/cm^3) [13]. If we use this threshold of lumbar BMD value as a criterion for osteoporosis diagnosis, the area under the ROC curve of thoracic BMD values would be 0.969, as shown in Figure 6. These results indicate that thoracic BMD values can also potentially replace lumbar BMD values for osteoporosis diagnosis. In routine clinical settings, especially for osteoporosis screening, high sensitivity is desired, which could be achieved by increasing the BMD threshold. For example, according to the above ROC curve, if the threshold of thoracic BMD value for osteoporosis diagnosis/screening is set to 150 mg/cm^3, the sensitivity for osteoporosis diagnosis can be 0.91, and the specificity is 0.89.

Figure 7 illustrates the variations in lumbar BMD among different racial groups. The median lumbar BMD values were 197 mg/cm^3, 188 mg/cm^3, 185 mg/cm^3 and 167 mg/cm^3 for Hispanic, Asian, Black and White. The results show that the median BMD values decrease sequentially from Hispanic to Asian to Black and finally to White, with Hispanics exhibiting the highest BMD and Whites the lowest.

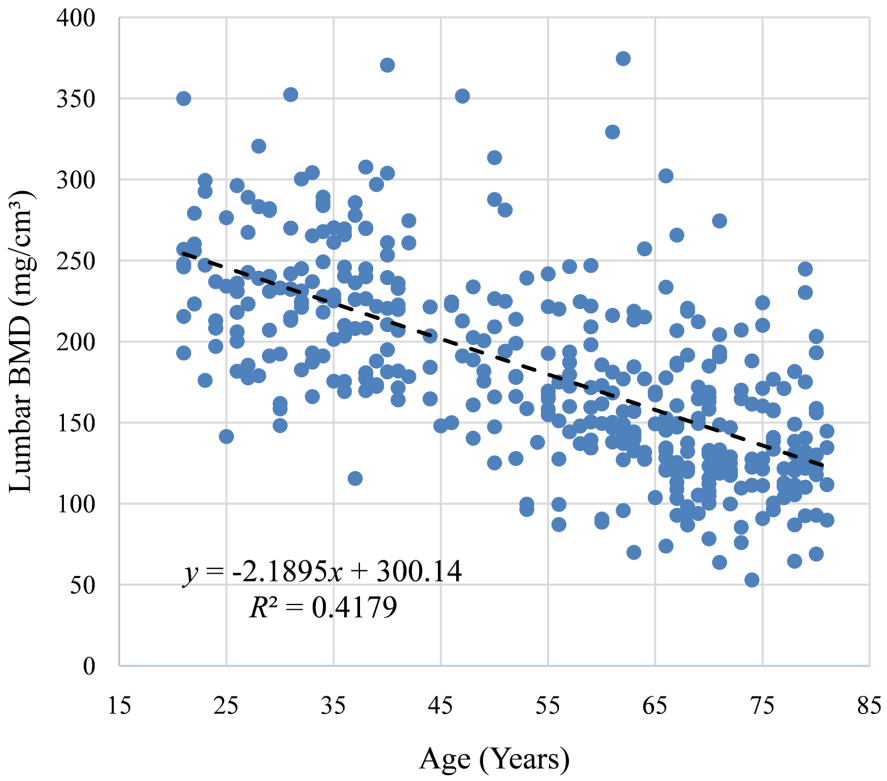

Figure 3. The results show that lumbar BMD values decreased with the subjects' ages, $r = -2.1895$, $p < 0.0001$.

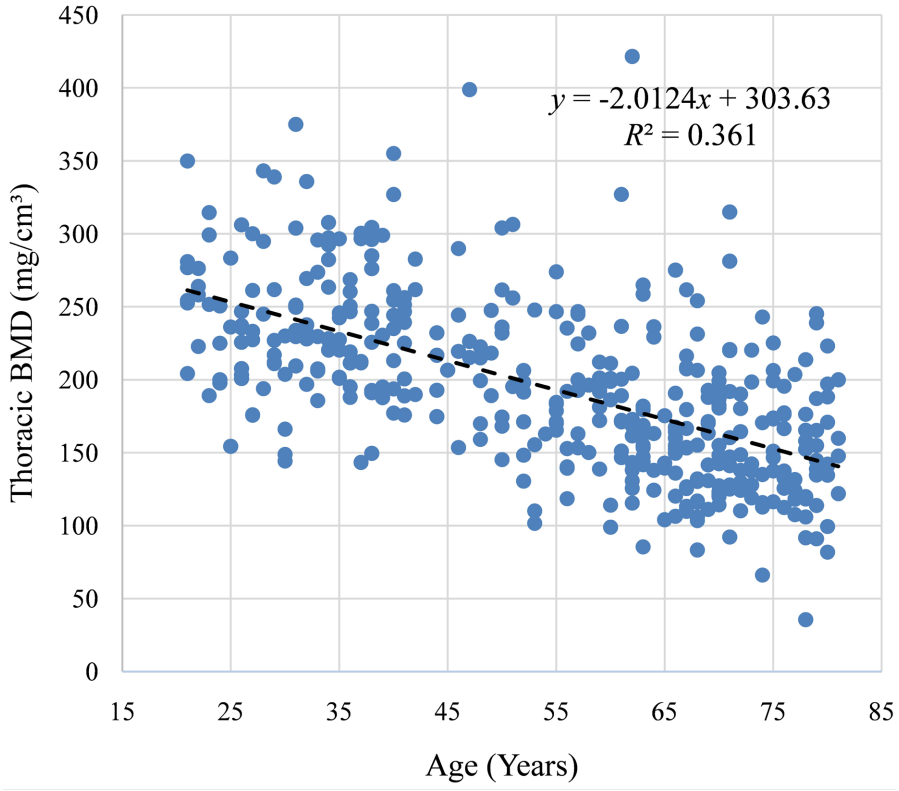

Figure 4. The results show that thoracic BMD values also decreased with the subjects' ages, $r = -2.012$, $p < 0.0001$.

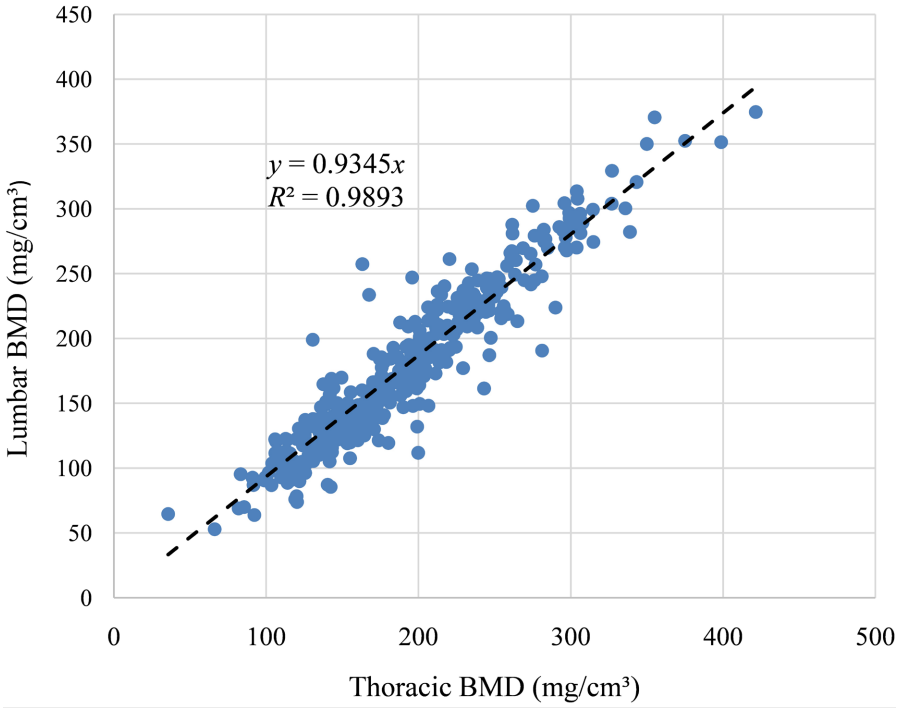

Figure 5. The Pearson correlation coefficient between thoracic and lumbar BMD is 0.953 ($p < 0.0001$), and linear regression line with zero intercept shows R-squared value = 0.9893.

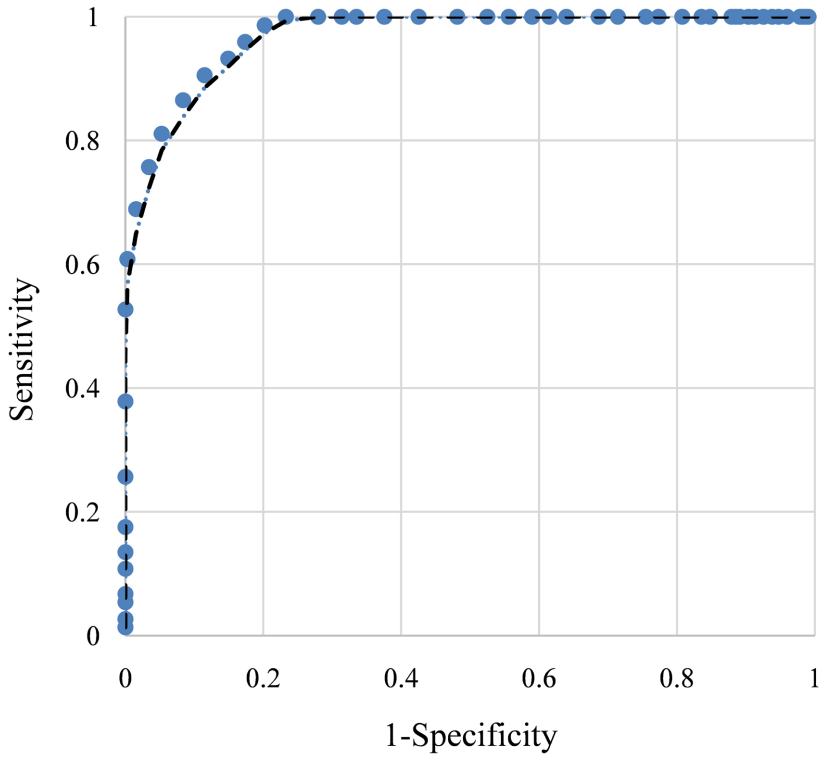

Figure 6. The area under the ROC curve of thoracic BMD is 0.969.

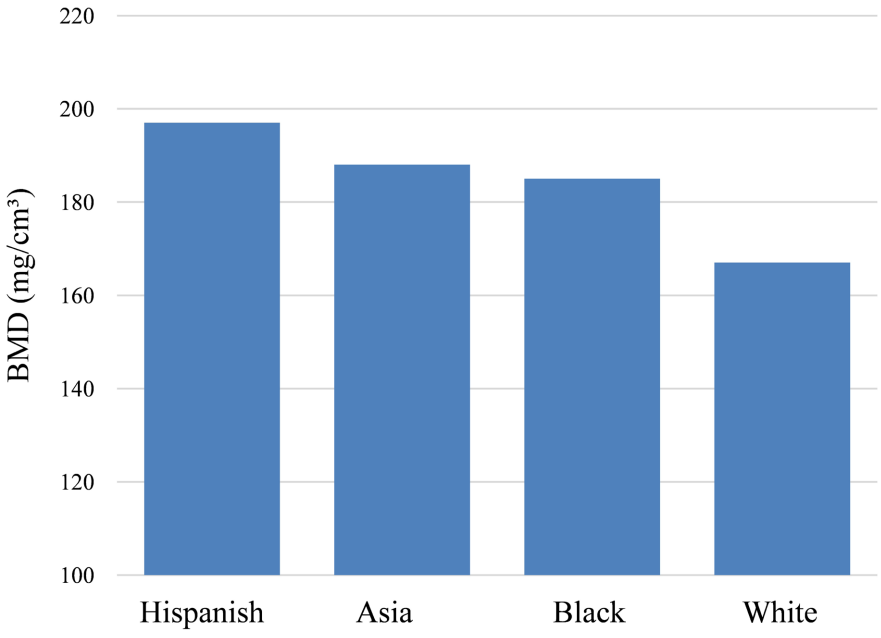

Figure 7. Lumbar BMD variations between different racial groups.

4. Discussion

Quantifying BMD is important to monitor and evaluate bone health status. Currently, dual-energy X-ray absorptiometry (DXA) is the gold standard for assessing BMD. However, it has a few drawbacks including spuriously elevated BMD

measurements in patients with degenerative disease, compression fractures, and vascular calcifications, which subsequently underestimates the risk of fractures. Measuring vertebral HU values on CT scans has been proposed as an alternate method of assessing BMD and bone quality [14]. The HU is a quantitative measurement of X-ray mass attenuation used by radiologists in the interpretation of CT images. Different tissue densities correlate with different HU values. The use of HU to objectively measure tissue densities has aided radiologists in the interpretation of CT images and diagnosis of disease and may also be used to assess bone quality and BMD [14] [15]. One study showed that thoracic and lumbar quantitative CTs provide a more sensitive method for detecting bone mineral loss when compared to DXA [16]. Furthermore, thoracic CT without contrast is commonly utilized for lung nodule and cancer screening. If this imaging modality can simultaneously assess bone health, it would significantly enhance the clinical value of these CT examinations, providing dual benefits for patients by detection of osteoporosis as well as the early detection of lung nodules and cancer.

Our study reveals variations in BMD among different racial groups, likely attributed to differences in diet, genetics, and lifestyle factors [17].

There are several reasons for choosing aortic blood and psoas muscle in our study: 1) Proximity to the spine: The aortic blood and psoas muscle are located adjacent to the lumbar spine, minimizing the impact of variations in beam hardening and scatter. This proximity ensures that the calibration accurately reflects the imaging conditions specific to the region of interest [8] [10]; 2) Consistent composition across subjects: Both aortic blood and psoas muscle exhibit relatively stable and predictable compositions, resulting in consistent HU values across individuals and imaging protocols. This consistency makes them suitable for calibration without the need for external phantoms [6] [8]; 3) Established use in literature: Previous studies have demonstrated the feasibility of using internal soft tissues for phantom-less calibration. For instance, Lee *et al.* [10] reported that aortic blood and psoas muscle provide reliable internal calibration metrics for BMD assessment, achieving high precision and reproducibility. Similarly, Therkildsen *et al.* highlighted the potential of internal calibration in routine clinical practice [9]; 4) Practical feasibility in routine clinical imaging: These tissues are routinely visualized in thoracic and abdominal CT scans, allowing opportunistic bone health assessment without additional imaging or radiation exposure [7] [12].

Current study focuses on primary osteoporosis, a condition where bone loss occurs due to the natural aging process. To accurately study primary osteoporosis, it is essential to select subjects who are as healthy as possible and free from conditions that might lead to secondary osteoporosis. Secondary osteoporosis is caused by various underlying diseases or conditions, which introduce significant changes in BMD independent of the aging process. The following explains the rationale for excluding these conditions: 1) Chronic Kidney Disease (CKD): CKD is a common cause of secondary osteoporosis due to renal osteodystrophy. It involves abnormalities in bone turnover, mineralization, and volume resulting from impaired

kidney function. CKD often leads to secondary hyperparathyroidism, altered vitamin D metabolism, and calcium-phosphate imbalances, all of which severely affect bone health and BMD [18]. Including patients with CKD could introduce pathological bone loss unrelated to primary osteoporosis; 2) Vitamin D Deficiency: Vitamin D plays a pivotal role in calcium absorption and bone mineralization. Severe deficiency leads to conditions like osteomalacia in adults, characterized by reduced BMD. Such variations, driven by a treatable deficiency rather than the natural aging process, could skew the study results [19]; 3) Long-Term Steroid Use: Glucocorticoids are well-known for inducing osteoporosis by decreasing bone formation and increasing bone resorption. Including patients on long-term steroids could confound BMD measurements, as the bone loss in such cases is pharmacologically induced rather than age-related; 4) Endocrine Disorders: Both hyperparathyroidism and hyperthyroidism significantly affect BMD and introduce systemic influences that could compromise the study's focus on primary osteoporosis; 5) Cirrhosis: Chronic liver disease contributes to hepatic osteodystrophy, which involves reduced bone formation and decreased BMD due to malnutrition, hypogonadism, and vitamin D metabolism abnormalities. These factors would confound the assessment of age-related bone loss; 6) Acute Leukemia and Diffuse Spinal Metastases: These conditions directly impact bone marrow and structural integrity, causing localized or diffuse changes in BMD unrelated to physiological aging. By excluding these diseases, which are common causes of secondary osteoporosis, the study ensures that the observed BMD variations are primarily due to the aging process. This approach helps isolate the natural progression of bone loss in healthy individuals, thereby improving the validity and reliability of the findings.

Despite the strong results validating the internal calibration techniques, it is still uncertain if these reference values are applicable across different subjects and across imaging protocols for opportunistic screening. Therefore, a broader approach for bone mineral density calibration is necessary to reduce the assumptions made by relying on these ground truth reference values.

5. Limitations

There are a few limitations in this study. First, we did not have lumbar BMD measurements by DXA, which is the consensus clinical standard to diagnose osteoporosis. In addition, the definition of the ROIs in spinal measurements is somewhat arbitrary. Second, our conclusions are limited to non-contrast scans. If intravenous contrast is used for chest and abdominal CT, some notable measurement bias in the thoracic and lumbar BMD could be observed [20]. Further investigations are needed to establish guidance for reliable use of thoracic and lumbar BMD in cases where CT scans include contrast agents.

6. Conclusion

A significant correlation was observed between thoracic and lumbar BMD values.

The correlation coefficient between thoracic and lumbar BMD was about 0.953. Both thoracic and lumbar BMD values decrease with the subjects' age. In addition, if the threshold lumbar BMD value of 123 mg/cm^3 is used as a criterion for osteoporosis diagnosis, the area under the ROC curve of thoracic BMD values is 0.969. These findings support the use of CT as a valuable tool in screening for osteoporosis based on thoracic and lumbar BMDs.

Conflicts of Interest

The authors declare no conflicts of interest regarding the publication of this paper.

References

[1] Shevroja, E., Lamy, O., Kohlmeier, L., Koromani, F., Rivadeneira, F. and Hans, D. (2017) Use of Trabecular Bone Score (TBS) as a Complementary Approach to Dual-Energy X-Ray Absorptiometry (DXA) for Fracture Risk Assessment in Clinical Practice. *Journal of Clinical Densitometry*, **20**, 334-345. https://doi.org/10.1016/j.jocd.2017.06.019

[2] WHO Study Group (1994) Assessment of Fracture Risk and Its Application to Screening for Postmenopausal Osteoporosis.

[3] Lin, J., Ines Boechat, M., G. Deville, J., Gilsanz, D., Stiehm, R., Gilsanz, V., *et al.* (2012) Quantitative Computerized Tomography (QCT) versus Dual X-Ray Absorptiometry (DXA) in the Assessment of Bone Mineral Density of HIV-1 Infected Children. *World Journal of AIDS*, **2**, 306-311. https://doi.org/10.4236/wja.2012.24041

[4] Stone, K.L., Seeley, D.G., Lui, L., Cauley, J.A., Ensrud, K., Browner, W.S., *et al.* (2003) BMD at Multiple Sites and Risk of Fracture of Multiple Types: Long-Term Results from the Study of Osteoporotic Fractures. *Journal of Bone and Mineral Research*, **18**, 1947-1954. https://doi.org/10.1359/jbmr.2003.18.11.1947

[5] Rice, J.C., Cowin, S.C. and Bowman, J.A. (1988) On the Dependence of the Elasticity and Strength of Cancellous Bone on Apparent Density. *Journal of Biomechanics*, **21**, 155-168. https://doi.org/10.1016/0021-9290(88)90008-5

[6] Engelke, K., Lang, T., Khosla, S., Qin, L., Zysset, P., Leslie, W.D., *et al.* (2015) Clinical Use of Quantitative Computed Tomography-Based Advanced Techniques in the Management of Osteoporosis in Adults: The 2015 ISCD Official Positions—Part III. *Journal of Clinical Densitometry*, **18**, 393-407. https://doi.org/10.1016/j.jocd.2015.06.010

[7] Weaver, A.A., Beavers, K.M., Hightower, R.C., Lynch, S.K., Miller, A.N. and Stitzel, J.D. (2015) Lumbar Bone Mineral Density Phantomless Computed Tomography Measurements and Correlation with Age and Fracture Incidence. *Traffic Injury Prevention*, **16**, S153-S160. https://doi.org/10.1080/15389588.2015.1054029

[8] Mueller, D.K., Kutscherenko, A., Bartel, H., Vlassenbroek, A., Ourednicek, P. and Erckenbrecht, J. (2011) Phantom-Less QCT BMD System as Screening Tool for Osteoporosis without Additional Radiation. *European Journal of Radiology*, **79**, 375-381. https://doi.org/10.1016/j.ejrad.2010.02.008

[9] Therkildsen, J., Thygesen, J., Winther, S., Svensson, M., Hauge, E., Böttcher, M., *et al.* (2018) Vertebral Bone Mineral Density Measured by Quantitative Computed Tomography with and without a Calibration Phantom: A Comparison between 2 Different Software Solutions. *Journal of Clinical Densitometry*, **21**, 367-374. https://doi.org/10.1016/j.jocd.2017.12.003

[10] Lee, D.C., Hoffmann, P.F., Kopperdahl, D.L. and Keaveny, T.M. (2017) Phantomless Calibration of CT Scans for Measurement of BMD and Bone Strength—Inter-Operator Reanalysis Precision. *Bone*, **103**, 325-333. https://doi.org/10.1016/j.bone.2017.07.029

[11] Bartenschlager, S., Dankerl, P., Chaudry, O., Uder, M. and Engelke, K. (2022) BMD Accuracy Errors Specific to Phantomless Calibration of CT Scans of the Lumbar Spine. *Bone*, **157**, Article ID: 116304. https://doi.org/10.1016/j.bone.2021.116304

[12] Johannesdottir, F., Allaire, B., Kopperdahl, D.L., Keaveny, T.M., Sigurdsson, S., Bredella, M.A., *et al.* (2020) Bone Density and Strength from Thoracic and Lumbar CT Scans Both Predict Incident Vertebral Fractures Independently of Fracture Location. *Osteoporosis International*, **32**, 261-269. https://doi.org/10.1007/s00198-020-05528-4

[13] American College of Radiology (2023) Performance of Quantitative Computed Tomography (QCT) Bone Mineral Density. https://www.acr.org/-/media/ACR/Files/Practice-Parameters/qct.pdf

[14] Zaidi, Q., Danisa, O.A. and Cheng, W. (2019) Measurement Techniques and Utility of Hounsfield Unit Values for Assessment of Bone Quality Prior to Spinal Instrumentation: A Review of Current Literature. *Spine*, **44**, E239-E244. https://doi.org/10.1097/brs.0000000000002813

[15] Narayanan, A., Cai, A., Xi, Y., Maalouf, N.M., Rubin, C. and Chhabra, A. (2019) CT Bone Density Analysis of Low-Impact Proximal Femur Fractures Using Hounsfield Units. *Clinical Imaging*, **57**, 15-20. https://doi.org/10.1016/j.clinimag.2019.04.009

[16] Mao, S.S., Li, D., Syed, Y.S., Gao, Y., Luo, Y., Flores, F., *et al.* (2017) Thoracic Quantitative Computed Tomography (QCT) Can Sensitively Monitor Bone Mineral Metabolism: Comparison of Thoracic QCT vs Lumbar QCT and Dual-Energy X-Ray Absorptiometry in Detection of Age-Relative Change in Bone Mineral Density. *Academic Radiology*, **24**, 1582-1587. https://doi.org/10.1016/j.acra.2017.06.013

[17] Hochberg, M. (2007) Racial Differences in Bone Strength. *Transactions of the American Clinical and Climatological Association*, **118**, 305-315.

[18] Levin, A., Bakris, G., Molitch, M., *et al.* (2007) Prevalence of Abnormal Bone and Mineral Metabolism in Chronic Kidney Disease Stages 1 to 3. *Clinical Journal of the American Society of Nephrology*, **2**, 373-381.

[19] Rosen, C.J., Abrams, S.A., Aloia, J.F., Brannon, P.M., Clinton, S.K., Durazo-Arvizu, R.A., *et al.* (2012) IOM Committee Members Respond to Endocrine Society Vitamin D Guideline. *The Journal of Clinical Endocrinology & Metabolism*, **97**, 1146-1152. https://doi.org/10.1210/jc.2011-2218

[20] Therkildsen, J., Winther, S., Nissen, L., Jørgensen, H.S., Thygesen, J., Ivarsen, P., *et al.* (2020) Feasibility of Opportunistic Screening for Low Thoracic Bone Mineral Density in Patients Referred for Routine Cardiac CT. *Journal of Clinical Densitometry*, **23**, 117-127. https://doi.org/10.1016/j.jocd.2018.12.002